

University of Massachusetts Amherst

From the Selected Works of Vincent Rotello

September 6, 2007

Integrated magnetic bionanocomposites through nanoparticle-mediated assembly of ferritin

S Srivastava
B Samanta
BJ Jordan
R Hong
Q Xiao, et al.



Available at: https://works.bepress.com/vincent_rotello/11/

Integrated Magnetic Bionanocomposites through Nanoparticle-Mediated Assembly of Ferritin

Sudhanshu Srivastava,[†] Bappaditya Samanta,[†] Brian J. Jordan,[†] Rui Hong,[†] Qijun Xiao,[‡] Mark T. Tuominen,[‡] and Vincent M. Rotello^{*†}

Contribution from the Departments of Chemistry and Physics, University of Massachusetts, Amherst, Massachusetts 01003

Received May 4, 2007; E-mail: rotello@chem.umass.edu

Abstract: Magnetic (FePt) and nonmagnetic (Au) nanoparticles were used to assemble ferritin into near-monodisperse bionanocomposites featuring regular interparticle spacing. The FePt/ferritin assemblies are integrated magnetic materials with ferritin providing added magnetic volume fraction to the magnetic nanocomposite. These assemblies differ from either of their constituent particles in terms of blocking temperature (T_B), net magnetic moment, coercivity, and remnance.

Introduction

Controlled synthesis and programmed assembly of magnetic nanoparticles provides a versatile approach to functional nanocomposite materials. These magnetic nanocomposites have been used for ultrahigh-density magnetic recording,¹ highly sensitive magnetic sensors,² magnetic separations,³ and nanocomposite permanent magnets.⁴ Further control of magnetic properties can be obtained by self-assembly of nanomagnets with nonmagnetic and magnetic materials. The magnetic properties of the resulting nanocomposite can be modulated through changes in the interparticle spacing⁵ and volume fraction of the magnetic material.⁶

Both polymers⁷ and biomolecules⁸ have been used extensively for the self-assembly of particles. The structure and recognition properties of biomolecules make them particularly attractive tools for self-assembly.⁹ Biomolecular assembly has likewise been applied to magnetic particles. Mann et al. used iron-containing magnetic proteins as inorganic nanoparticles¹⁰ for

the assembly process using streptavidin/biotin binding. Similarly, Weissleder et al. showed viral-induced assembly of magnetic nanoparticles,¹¹ while we demonstrated electrostatic assembly of particles using DNA.¹² To date, however, magnetically active biomolecular and synthetic systems have not been combined to create integrated magnetic materials.

Ferritin provides a particularly attractive magnetic biomaterial. Ferritin is an iron storage protein that features a protein shell surrounding an iron oxide core consisting of ~4500 Fe atoms (6 nm core, 12 nm overall).¹³ Apoferritin has also been used to provide nanoparticles featuring a variety of magnetic and nonmagnetic materials.¹⁴ We report here the self-assembly of ferritin by magnetic nanoparticles as a modular approach to the creation of integrated magnetic nanocomposites (Scheme 1). In these materials the magnetic dipoles of the synthetic and biological components interact, as manifested by changes in the blocking temperature (T_B), net magnetic moment, remanance, and coercivity of the resulting composites.

Results and Discussion

Ferritin is an anionic protein with a pI of 4.5.¹⁵ Electrostatic complementarity was provided through functionalization of

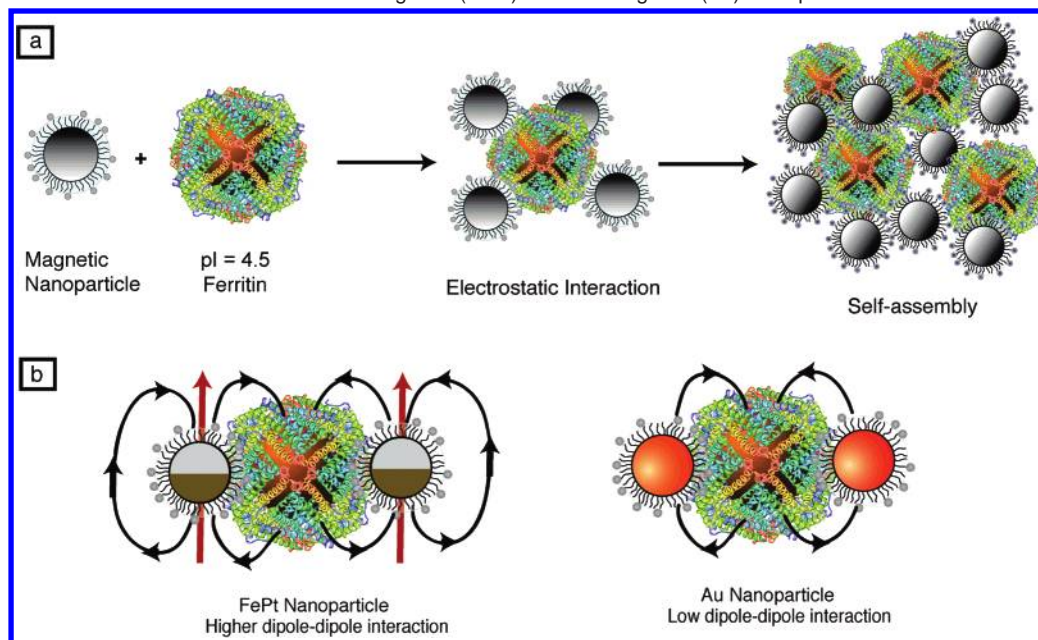
[†] Department of Chemistry.

[‡] Department of Physics.

- (1) (a) Metzger, R. M.; Kononov, V. V.; Sun, M.; Xu, T.; Zangari, G.; Xu, B.; Benakli, M.; Doyle, W. D. *IEEE Trans. Magn.* **2000**, *36*, 30–35. (b) Sun, M.; Zangari, G.; Shamsuzzoha, M.; Metzger, R. M. *Appl. Phys. Lett.* **2001**, *78*, 2964–2966.
- (2) Elliott, C. M.; Steiner, U. E.; Kremer, J. J.; Hotzer, K. A. *Chem. Mater.* **2005**, *17*, 941–943.
- (3) Wang, D.; He, J.; Rosenzweig, N.; Rosenzweig, Z. *Nano Lett.* **2004**, *4*, 409–413.
- (4) Yue, B.; Lee, E. D.; Rockwood, A. L.; Lee, M. L. *Anal. Chem.* **2005**, *77*, 4160–4166.
- (5) Vestal, C. R.; Song, Q.; Zhang, Z. J. *J. Phys. Chem. B* **2004**, *108*, 18222–18227.
- (6) Tartaj, P.; Gonzalez-Carreno, T.; Serna, C. J. *J. Phys. Chem. B* **2003**, *107*, 20–24.
- (7) (a) Fendler, J. H. *Chem. Mater.* **1996**, *8*, 1616–1624. (b) Shenhar, R.; Rotello, V. M. *Acc. Chem. Res.* **2003**, *36*, 549–561. (c) Boal, A. K.; Ilhan, F.; DeRouchey, J. E.; Thurn-Albrecht, T.; Russell, T. P.; Rotello, V. M. *Nature* **2000**, *404*, 746–748.
- (8) (a) Niemeyer, C. M. *Angew. Chem., Int. Ed.* **2001**, *40*, 4128–4158. (b) Kim, T.; Rajan, K.; Shima, M. *IEEE Trans. Nano Biosci.* **2006**, *5*, 210–214. (c) Mirkin, C. A.; Letsinger, R. L.; Mucic, R. C.; Storhoff, J. J. *Nature* **1996**, *382*, 607–609. (d) Kim, T.; Reis, L.; Rajan, K.; Shima, M. *J. Magn. Mater.* **2005**, *295*, 132–138. (e) Shenton, W.; Pum, D.; Sleytr, U. B.; Mann, S. *Nature* **1997**, *389*, 585–587.

- (9) (a) Haes, A. J.; VanDuyne, R. P. *J. Am. Chem. Soc.* **2002**, *124*, 10596–10604. (b) Wang, S. P.; Mamedova, N.; Kotov, N. A.; Chen, W.; Studer, J. *Nano Lett.* **2002**, *2*, 817–822. (c) Srivastava, S.; Verma, A.; Frankamp, B. L.; Rotello, V. M. *Adv. Mater.* **2005**, *17*, 617–621. (d) Verma, A.; Srivastava, S.; Rotello, V. M. *Chem. Mater.* **2005**, *17*, 6317–6322. (e) Alivisatos, A. P.; Johnsson, K. P.; Peng, X. G.; Wilson, T. E.; Loweth, C. J.; Bruchez, M. P.; Schultz, P. G. *Nature* **1996**, *382*, 609–611.
- (10) Li, M.; Wong, K. K. W.; Mann, S. *Chem. Mater.* **1999**, *11*, 23–26.
- (11) Perez, J. M.; Simeone, F. J.; Saeki, Y.; Josephson, L.; Weissleder, R. *J. Am. Chem. Soc.* **2003**, *125*, 10192–10193.
- (12) Srivastava, S.; Samanta, B.; Arumugam, P.; Han, G.; Rotello, V. M. *J. Mater. Chem.* **2007**, *17*, 52–55.
- (13) (a) Jin, W.; Takagi, H.; Pancorbo, B.; Theil, E. C. *Biochemistry* **2001**, *40*, 7525–7532. (b) Douglas, T.; Stark, V. T. *Inorg. Chem.* **2000**, *39*, 1828–1830. (c) Brem, F.; Tiefenauer, L.; Fink, A.; Dobson, J.; Hirt, A. M. *Phys. Rev. B* **2006**, *73*, 224427(1–6). (d) Makhlof, S. A.; Parker, F. T.; Berkowitz, A. E. *Phys. Rev. B* **1997**, *55*, R14717–720.
- (14) (a) Okuda, M.; Iwahori, K.; Yamashita, I.; Yoshimura, H. *Biotechnol. Bioeng.* **2003**, *82*, 187–194. (b) Kramer, R. M.; Li, C.; Carter, D. C.; Stone, M. O.; Naik, R. R. *J. Am. Chem. Soc.* **2004**, *126*, 13282–13286.
- (15) (a) Kato, T.; Shimada, T. *J. Biochem.* **1970**, *68*, 681–687. (b) Cohen, S.; Vernier, R. L.; Michael, A. F. *Am. J. Pathol.* **1983**, *110*, 170–181.

Scheme 1. (a) Magnetic Nanoparticles Assembled with Ferritin via Electrostatic Interaction; (b) Schematic Representation of Magnetic Dipole–Dipole Interaction of Ferritin Assembled with Magnetic (FePt) and Nonmagnetic (Au) Nanoparticles



nanoparticles with cationic trimethylammonium ligands. FePt nanoparticle (NP **1**) (8 nm) was fabricated as reported using lauric acid and lauryl amine as capping ligands.¹⁶ Water solubility and cationic charge were obtained through place exchange using thioalkylated oligo(ethylene glycol) with trimethyl ammonium chain-end ligands (Figure 1),¹⁷ providing a particle with a zeta potential of +25 mV in Tris buffer. Similarly, an Au nanoparticle (~6.5 nm core) was fabricated as previously reported¹⁸ from the undecanethiol-functionalized precursor and place exchanged with 11-mercapto undecyltrimethylammonium ligand to afford NP **2** (zeta potential +30 mV).¹⁹

The assembly process was achieved through slow addition of nanoparticles **1** and **2** to a solution of ferritin with a final stoichiometry of 1:10. The assembly of nanoparticles with ferritin in solution was initially analyzed via dynamic light scattering (DLS) (see Supporting Information).²⁰ Ferritin had a bimodal peak (~15 and 59 nm); presumably, the second peak is due to protein–protein interactions (zeta potential –28 mV). Upon addition of nanoparticles substantially larger aggregates were formed. These aggregates were nearly monodisperse with 150 ± 2 nm assemblies observed with NP **1** (zeta potential –2 mV) and 100 ± 6 nm aggregates (zeta potential –10 mV) observed with NP **2** (Figure 2e).²¹

The regularity of the aggregate sizes was verified by TEM. Precipitation was observed over time for both of the assemblies. ImageJ software was used to quantify the sizes of these aggregates demonstrated by TEM²² with dispersities for NP **1**

(125 ± 7 nm) and **2** (90 ± 9 nm) comparable to those observed using DLS (Figure 2).²³ The smaller size of the aggregates presumably arises from shrinkage of the assemblies upon drying.

The interparticle spacing of the aggregates was quantified through small-angle X-ray scattering (SAXS, Figure 3) after precipitation of the aggregates and drop casting of the nanoparticles alone onto mylar sheets. The q values, representative of average interparticle spacing, shift steadily downward in the presence of ferritin, indicating an increase in interparticle spacing. As an example, the drop-cast film of NP **1** alone has a center-to-center spacing of 11.1 nm, while that of the ferritin alone is 8.6 nm. Upon assembly of NP **1** with ferritin the center-to-center spacing increases to 18.9 nm.²⁴ Similar ~8 nm increase in spacing was observed with NP **2** upon assembly with ferritin.

Field-dependent magnetization analysis using zero-field-cooled (ZFC) and field-cooled (FC) measurements for ferritin, nanoparticles, and assembled nanocomposites were performed using a superconducting quantum interference device (SQUID). Ferritin and nanoparticles were superparamagnetic at ambient temperature²⁵ with the transition to ferromagnetic behavior (i.e., blocking temperature, T_B)²⁶ occurring at 15 K for ferritin, Table 1. The control sample of NP **1** without ferritin had a T_B of 94 K, while the ferritin/NP **1** assembly showed an increase in T_B to 105 K (Figure 4). This behavior is opposite to the decrease in T_B observed when particles are assembled with nonmagnetic materials.^{12,27} The increase in blocking temperature can be

(16) Chen, M.; Liu, J. P.; Sun, S. *J. Am. Chem. Soc.* **2004**, *126*, 8394–8395.

(17) Hong, R.; Fischer, N. O.; Emrick, T.; Rotello, V. M. *Chem. Mater.* **2005**, *17*, 4617–4621.

(18) Carroll, J. B.; Frankamp, B. L.; Srivastava, S.; Rotello, V. M. *J. Mater. Chem.* **2004**, *14*, 690–694.

(19) Teranishi, T.; Hasegawa, S.; Shimizu, T.; Miyake, M. *Adv. Mater.* **2001**, *13*, 1699–1701.

(20) Schmidt, V.; Giacomelli, C.; Lecolley, F.; Lai-Kee-Him, J.; Brisson, A. R.; Borsali, R. *J. Am. Chem. Soc.* **2006**, *128*, 9010–9011.

(21) As the molar ratio was 1:10 (NP:Ferritin), and ferritin was in excess compared to NPs. The zeta potential values remained negative for the nanocomposites of NP **1**/ferritin (–2 mV) and NP **2**/ferritin (–10 mV) compared to ferritin alone (–28 mV).

(22) Rasband, W. S. *ImageJ*; U.S. National Institutes of Health, Bethesda, MD, 1997–2006; <http://rsb.info.nih.gov/ij/>.

(23) (a) Naka, K.; Itoh, H.; Chujo, Y. *Nano Lett.* **2002**, *2*, 1183–1186. (b) Zhou, Y.; Antonietti, M. *J. Am. Chem. Soc.* **2003**, *125*, 14960–14961. (c) Li, X.; Li, Y.; Tan, Y.; Yang, C.; Li, Y. *J. Phys. Chem. B* **2004**, *108*, 5192–5199.

(24) The peak denotes the spacing between two nanoparticles spaced by ferritin and a secondary shoulder peak presenting the spacing between ferritin and nanoparticle.

(25) For superparamagnetic state the thermal energy $k_B T$ is large enough to produce rapid fluctuations and cross the energy barrier for magnetization reversal, which leads to a time-averaged magnetization of zero-termed superparamagnetic relaxation.

(26) For noninteracting particles the energy barrier is determined by the intrinsic anisotropy density and the volume of the nanoparticle. $T_B \approx k_i V/30K$ serves as a practical definition of blocking temperature for a measurement time of ~1000 s.

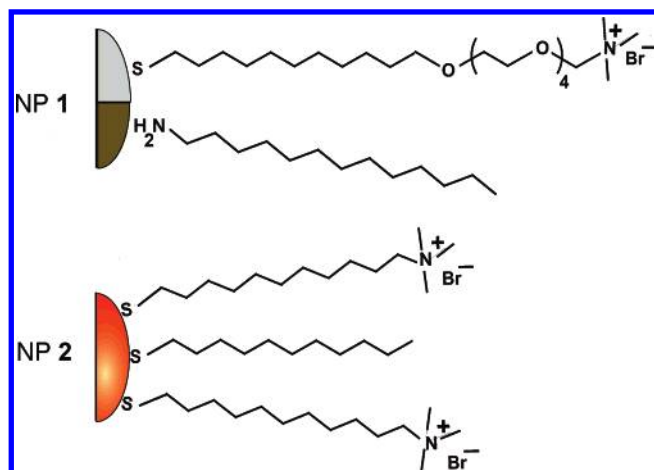


Figure 1. Schematic structure of FePt (NP 1) and Au (NP 2) after place exchange reactions.

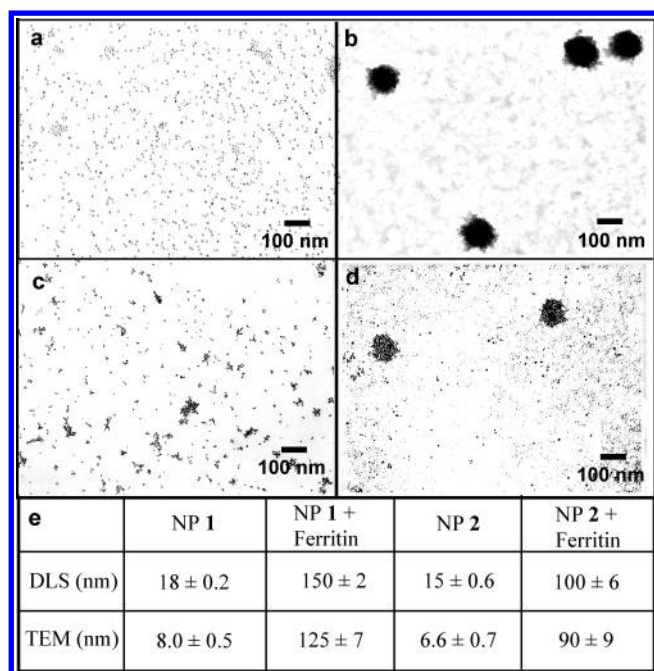


Figure 2. TEM of (a) NP 1 and (b) NP 1-ferritin nanocomposites and (c) NP 2 and (d) NP 2-ferritin nanocomposites. (e) Mean average hydrodynamic diameter with the standard deviation of the distribution for NP 1, 2, and their respective assemblies in solution and aggregate diameter of dried assemblies as determined by DLS and TEM.

Table 1. Summary of the Magnetic Studies Carried out for NP 1, 2 with Respective Assemblies

	blocking temp., T_B (K)	coercivity, H_C (Oe) ^a	reduced rem., H_R (emu) ^a	magnetic moment, μ (emu/g) ^b
NP 1	94	450	0.47	16.9
NP 1 + ferritin	105	520	0.32	21.4
NP 2 + ferritin	15	1800	0.12	1.2
ferritin	15	1800	0.12	1.8

^a Values obtained at 5 K. ^b Obtained at 1.8 K.

explained by a local increase in the density of the magnetic material in the nanocomposites. While ferritin increases interparticle spacing, the magnetic core of the protein appears to

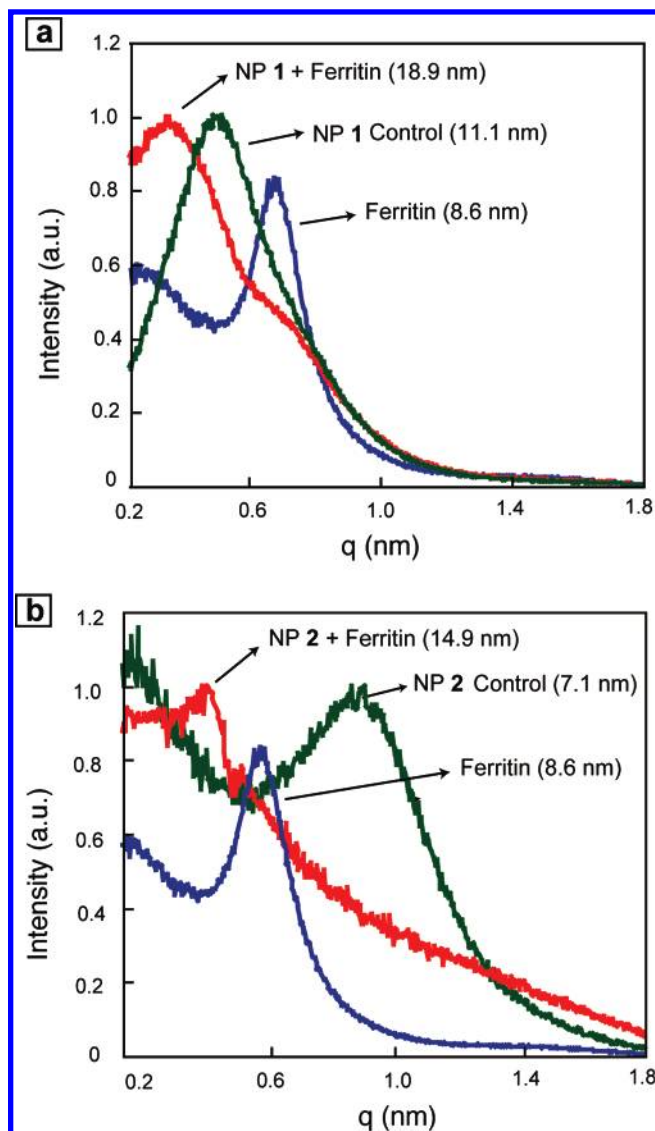


Figure 3. SAXS of ferritin and assemblies: (a) NP 1 and NP 1-ferritin nanocomposites, (b) NP 2 and NP 2-ferritin nanocomposites.

enhance the magnetic interaction between nanoparticles by either a dipolar²⁸ or exchange²⁹ mechanism. The observed increase in T_B by ~ 12 K is therefore a direct consequence of the ferritin-mediated assembly: the interparticle coupling and ferritin core combine to provide an effective increase in magnetic volume compared to the control sample.^{5,6} As a control, diamagnetic NP 2 exerted no change on the T_B of the ferritin, indicating that the ferritin is effectively uncoupled in both its native state and after assembly with NP 2.

Field-dependent magnetization studies were obtained on films of NP 1 alone and NP 1 assembled with ferritin. Hysteresis plots offer a view into the collective behavior of NP 1 and ferritin systems, providing values of magnetic remanence (M_R) and coercivity (H_C).²⁷ At low-temperature hysteretic behavior was observed in all cases, and the plots are shown in Figure 5. The remanent magnetization factor for NP 1 alone was 0.47

(27) (a) Frankamp, B. L.; Boal, A. K.; Tuominen, M. T.; Rotello, V. M. *J. Am. Chem. Soc.* **2005**, *127*, 9731–9735. (b) Boal, A. K.; Frankamp, B. L.; Uzun, O.; Tuominen, M. T.; Rotello, V. M. *Chem. Mater.* **2004**, *16*, 3252–3256.

(28) (a) Farrell, D.; Cheng, Y. H.; Ding, Y.; Yamamuro, S.; Sanchez-Hanke, C.; Kao, C. C.; Majetich, S. A. *J. Magn. Magn. Mater.* **2004**, *282*, 1–5. (b) Farrell, D.; Ding, Y.; Majetich, S. A.; Sanchez-Hanke, C.; Kao, C. C. *J. Appl. Phys.* **2004**, *95*, 6636–6638.

(29) Zeng, H.; Li, J.; Liu, J. P.; Wang, Z. L.; Sun, S. *Nature* **2002**, *420*, 395–398.

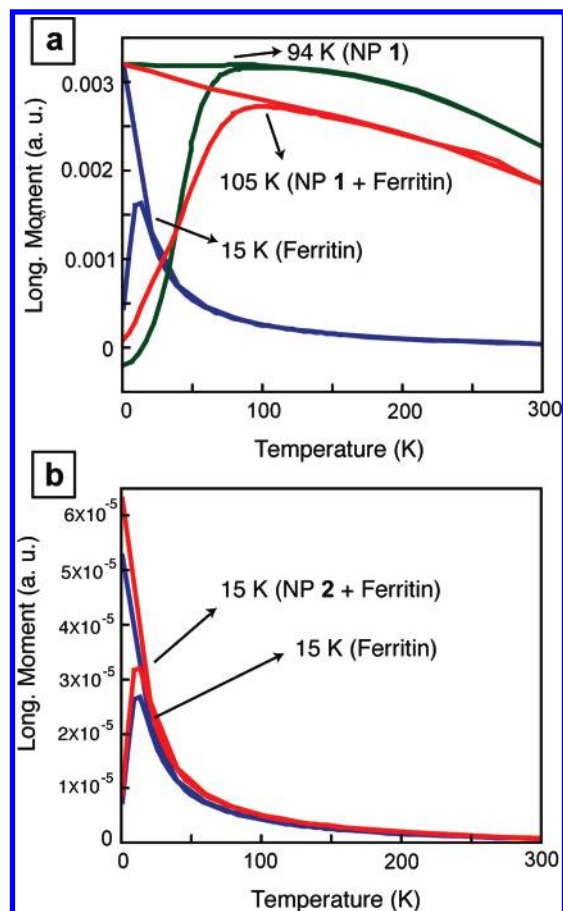


Figure 4. SQUID results for (a) ferritin, NP 1 and NP 1-ferritin nanocomposites and (b) ferritin and NP 2-ferritin nanocomposites.

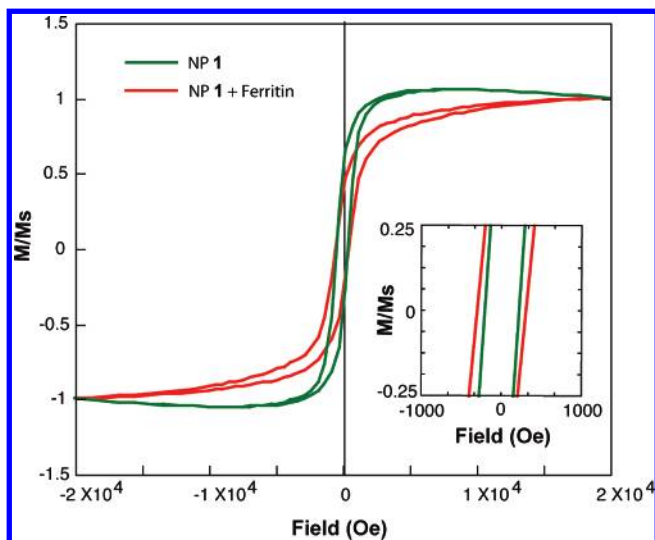


Figure 5. Field sweep hysteresis plot (5 K) of NP 1 and NP 1 assembled with ferritin. Plots are normalized to saturation magnetization.

emu, while the ferritin-assembled NP 1 showed a lower value of 0.32 emu. The coercivity calculated from the plot of the assembled particles was found to be ~ 520 Oe, while the control showed a smaller value of 450 Oe. The increased coercivity observed with the ferritin-assembled NP 1 arises from the enhanced coupling between the dipoles of ferritin and NP 1 leading to a harder magnetic material. Likewise, the stronger dipolar coupling between the dipoles of ferritin and NP 1 lowers the remanance by inducing a greater degree of frustration in

the sample.³⁰ As expected, the hysteresis curves for the gold NPs as a control showed no change in the curves compared to ferritin alone (Supporting Information).

To investigate the effect of volume fraction on T_B , the net magnetic moment for each sample was also determined. In this experiment the same amount of nanoparticles alone and nanoparticles assembled with ferritin were introduced to a constant 20 000 Oe field at 300 K and cooled to 1.8 K in the presence of field.³¹ NP 1 alone gave 16.9 emu/g, while NP 1 assembled with ferritin gave a moment of 21.4 emu/g. These results support the enhancement in the volume fraction and the change in T_B of the bionanocomposite.³² In contrast, NP 2 assembled with ferritin showed a lower magnetic moment (1.2 emu/g) in comparison to ferritin (1.8 emu/g) as more diamagnetic material was added to the nanocomposite.³³

Conclusion

In summary, we demonstrated the fabrication of bionanocomposites based on ferritin and synthetic nanoparticles. This assembly process provided discrete essentially monodisperse aggregates (as determined by DLS and TEM) that feature controlled interparticle spacing. Most significantly, this assembly strategy provides nanocomposites where the structural components are also functional, yielding a highly modular approach to biomagnetic materials.

Experimental Section

Materials. Ferritin from horse spleen was purchased from Sigma. All other starting materials were purchased from Sigma-Aldrich Chemical Co. except iron pentacarbonyl and dodecylamine. The later chemicals were purchased from Acros Chemical Co. and used without further purification. MilliQ water and ethanol solvents were also used without further purification. A Digi-Sense Temperature controller R/S (model 68900-11) was used to control the temperature.

Synthesis of Trimethylammonium-Functionalized FePt Nanoparticles^{16,17} (NP 1). Magnetic FePt nanoparticles were synthesized through thermal decomposition of $\text{Pt}(\text{acac})_2$ and $\text{Fe}(\text{CO})_5$ in hot organic solvents using the reported procedure with minor modifications. Lauric acid and dodecyl amine were used as capping ligands for generating the core, and the detailed procedure is reported in the Supporting Information. For place exchange 30 mg of FePt nanocrystals was taken in 5 mL of dichloromethane. A 80 mg amount of (thiol ligand) SH-C₁₁-tetra(ethylene glycol)lyated trimethylammonium bromide in 0.5 mL of ethanol was added to the nanocrystals dispersion and stirred for 3 days. The black precipitate obtained was isolated using centrifugation. It was washed three times using a mixture of ethanol and dichloromethane (1:10) and dissolved in MilliQ water.

Synthesis of Trimethylammonium-Functionalized Gold Nanoparticles (NP 2). Synthesis of the nanoparticles core was carried out based on the reported procedure.¹⁸ For the place exchange reaction 10 mg of gold nanocrystals was taken in 5 mL of toluene. A 50 mg amount of 11-mercapto undecyltrimethylammonium bromide in 0.5 mL of dichloromethane was added to the nanocrystals dispersion and stirred for 1 day. The black precipitate was then washed three times using dichloromethane and dissolved in MilliQ water.

(30) Held, G. A.; Grinstein, G.; Doyle, H.; Sun, S.; Murray, C. B. *Phys. Rev. B* **2001**, *64*, 012408(1–4).

(31) Same amount of nanoparticles were added in each sample of nanoparticles alone and their respective assemblies with ferritin.

(32) A similar study was carried out with Fe_3O_4 nanoparticles with ferritin giving 5K enhancement in T_B as reported in the Supporting Information.

(33) In the case of Au nanoparticles the same amount of ferritin was added to ferritin as control and the assembled nanocomposite of Au. The results showed a smaller magnetic moment for the assembly (1.2 emu/g) in comparison to ferritin alone (1.8 emu/g) at 6 T due to more diamagnetic material (Au) being added.

Dynamic Scattering Light (DLS). DLS experiments were performed on a Malvern Zetasizer Nano ZS using a quartz cuvette with a 10 mm path length. Samples for DLS were prepared by adding NPs ($0.5 \mu\text{M}$ in water) drop by drop to ferritin solution ($5 \mu\text{M}$ in water) in a 1:10 molar ratio. The samples were analyzed after 15 min and 24 h of incubation. For zeta potential analysis, all the nanoparticles ($0.5 \mu\text{M}$), ferritin alone ($0.5 \mu\text{M}$), and nanocomposites in 1:10 (NP:ferritin) molar ratio were analyzed in 5 mM Tris(hydroxymethyl)aminomethane buffer at pH 7.4.

Transmission Electron Microscopy (TEM). A drop of the turbid solution of the precipitate of NP+ferritin assembly was placed on a 300-mesh carbon-coated Cu grid. The samples were then examined on JEOL 2000 *fx* operating at 200 keV TEM.

Small-Angle X-ray Scattering (SAXS). Samples for SAXS analysis were prepared by placing a $\sim 1 \text{ cm}^2$ piece of Mylar film at the bottom of a 2 mL vial that contains ferritin solution. NPs ($5 \mu\text{M}$ in water) were added drop by drop to ferritin solution ($50 \mu\text{M}$ in water) in a 1:10 molar ratio. The samples were allowed to fully precipitate. The remaining solution was then removed, and the samples were dried completely under air.

Superconducting Quantum Interference Device (SQUID). Thin films were prepared identical to SAXS samples and analyzed under SQUID. Data were acquired on a Quantum Design SQUID Magnetometer. ZFC-FC plots were acquired by cooling the sample to 1.8 K in the absence of a magnetic field, and then a field of 100 Oe was applied. Then the sample was slowly warmed to 300 K and returned

to 1.8 K, thus acquiring FC and ZFC plots in a single temperature sweep. Field sweep measurements were taken at a temperature of 5 K, sweeping from 20 000 to $-20\,000$ Oe and back for NP **1** and similarly 60 000 to $-60\,000$ Oe and back for ferritin. For magnetic moment studies each sample was dried completely and weighed on mylar sheets. An equal amount of nanoparticles was added for each sample to calculate the magnetic moment. Each sample was allowed to cool from 300 to 1.8 K in the presence of 2 and 6 T magnetic field for saturating the system, and then RSO centering was carried out to calculate the magnetic moment in emu/g.

Acknowledgment. This research was supported by the National Science Foundation (CHE-0518487, MRSEC facilities, and the Center for Hierarchical Manufacturing, DMI-0531171) and Keck Foundation. B.J.J. also acknowledges a NSF IGERT fellowship (DUE-044852).

Supporting Information Available: TEM, SAXS, and SQUID results for iron oxide nanoparticles assembled with ferritin are compared; circular dichroism (CD) study for FePt particles and all the DLS profiles of the NPs, ferritin, and their respective assemblies; hysteresis curves for ferritin and ferritin assembled gold particles. This material is available free of charge via the Internet at <http://pubs.acs.org>.

JA073163X